

## Research Article

# Development an Artificial Neural Network Model for Estimating Cost of R/C Building by Using Life-Cycle Cost Function: Case Study of Mexico City

Henry E. Reyes,<sup>1</sup> Juan Bojórquez ,<sup>1</sup> Laura Cruz-Reyes,<sup>2</sup> Sonia E. Ruiz ,<sup>3</sup> Alfredo Reyes-Salazar,<sup>1</sup> Edén Bojórquez ,<sup>1</sup> Manuel Barraza ,<sup>4</sup> Antonio Formisano,<sup>5</sup> Omar Payán ,<sup>6</sup> and José R. Torres<sup>6</sup>

<sup>1</sup>Facultad de Ingeniería, Universidad Autónoma de Sinaloa, Culiacán 80013, Mexico

<sup>2</sup>Instituto Tecnológico de Ciudad Madero, Ciudad Madero, Tamaulipas, Mexico

<sup>3</sup>Instituto de Ingeniería, Universidad Nacional Autónoma de México, Coyoacán 04510, Mexico

<sup>4</sup>Facultad de Ingeniería, Arquitectura y Diseño, Universidad Autónoma de Baja California, Ensenada 22860, Mexico

<sup>5</sup>Department of Structures for Engineering and Architecture, University of Naples, Naples 80125, Italy

<sup>6</sup>Department of Mechanical and Mechatronic Engineering, Tecnológico Nacional de México, Culiacán, Sinaloa, Mexico

Correspondence should be addressed to Juan Bojórquez; [juanbm@uas.edu.mx](mailto:juanbm@uas.edu.mx), Edén Bojórquez; [eden@uas.edu.mx](mailto:eden@uas.edu.mx), Manuel Barraza; [barraza.manuel@uabc.edu.mx](mailto:barraza.manuel@uabc.edu.mx), and Omar Payán; [omarjps@hotmail.com](mailto:omarjps@hotmail.com)

Received 27 January 2022; Revised 10 March 2022; Accepted 13 March 2022; Published 12 April 2022

Academic Editor: Qian Chen

Copyright © 2022 Henry E. Reyes et al. This is an open access article distributed under the Creative Commons Attribution License, which permits unrestricted use, distribution, and reproduction in any medium, provided the original work is properly cited.

This paper addresses the importance of engineering asset management decisions and control. For this purpose, a Life-Cycle Cost (LCC) analysis is conducted for typical reinforced concrete (R/C) buildings located in Mexico City. The objective of this study is to develop an artificial neural network (ANN) model that can estimate the total expected cost of R/C buildings by using LCC functions. The total cost includes the initial cost and the cost of the damage caused by future possible ground motions at the site of interest. The present value of the cost includes: initial cost, repair or reconstruction cost, cost of damage to the contents, costs associated with the loss of life or injuries and economic losses. The structural performance is evaluated using probabilistic models, artificial neural networks models are used to obtain the seismic response of the buildings. The methodology is applied to a set of reinforced concrete buildings with 4, 8, and 12 stories which are located at the soft soil of Mexico City. Finally, it is concluded that the life-cycle cost is efficiently obtained using artificial neural network models for estimating the structural reliability of reinforced concrete buildings, in such a way that it can be used as an excellent planning tool that covers long spans of time.

## 1. Introduction

The life-cycle cost estimation has received abundant attention over the past decades. In that time, the challenge of estimating the total life-cycle costs of structures considering all variables involved in the problem has represented a difficult task. There is a vast amount of literature available regarding the estimation of the expected cost for different structural systems [1–19]; however, those studies generally are applied to a limited number of particular cases. Furthermore, one of the main limitations of those studies is the

time consuming of the methodology to obtain the total expected cost. This study addresses this issue, to perform this task artificial neural networks are used aiming to minimize the time consuming of the methodology within low errors in the estimation. The great potential of ANNs is the high-speed processing provided in a massive parallel implementation [20]. ANNs can be developed and used for image recognition, natural language processing and so on. Nowadays, ANNs are vastly used for universal function approximation in numerical paradigms because of their excellent properties of self-learning, adaptivity, fault

tolerance, nonlinearity, and advancement in input and output mapping [21]. In the engineering field ANN has been used for optimization and seismic code calibration [22], they have been applied for estimating concrete and reinforcement consumption in the construction of integral bridges [23]; moreover, an artificial neural network model has been applied to estimate the construction costs [24]. For bridge design an ANN was used to decrease the computational demand of box-girder element analysis [25]. The prediction and identification of seismic-induced damage in structures has been possible using neural networks [26–28]. For earthquake engineering, the use of the power of ANN pattern recognition was applied to evaluate seismic risk problems [29].

The estimation of the life-cycle cost of buildings is a primary part of a construction project, it is considered one of the major criteria in building design for its importance in helping to choose economic structural configurations and to estimate future costs of ownership. In this paper, it is considered that the total expected life-cycle cost of buildings includes: the initial costs plus the expected costs of the damage caused to the structure by future earthquakes, including repair cost, cost of damage to the contents, the cost associated with the loss of life and injuries, and direct economic losses [30]. The loads considered for the structural design are: dead load, life load, and earthquake loads. The structural performance is evaluated using probabilistic analysis. The occurrence of earthquakes is described by a Poisson process [31]. The methodology is applied to a set of reinforced concrete buildings with 4, 8, and 12 stories (low, middle and high rise) located in soft soil with ground period of  $T_s = 2.0s$  of Mexico City, which are of main concern in Mexico City Building Code (MCBC). Finally, it is concluded that artificial intelligence can provide accurate results, minimize prediction errors, and it can be used as an excellent planning tool that covers long spans of time.

## 2. General Methodology

The general approach taken to obtain the life-cycle costs of buildings is summarized in the steps below and illustrated in Figure 1.

**2.1. Structural Design of Buildings (Step 1).** The buildings are designed according to the Mexico City Building Code considering the seismic design and concrete regulations for buildings located in the soft soil of Mexico City.

**2.2. Maximum Structural Capacity (Step 2).** The maximum structural capacity is obtained using incremental dynamic analysis (IDA) [32]. For this aim, the maximum inter-story drift (MID) is selected as the engineering demand parameter to conduct the analysis. The associated yielding and near collapse limit states of the buildings can be obtained from this analysis.

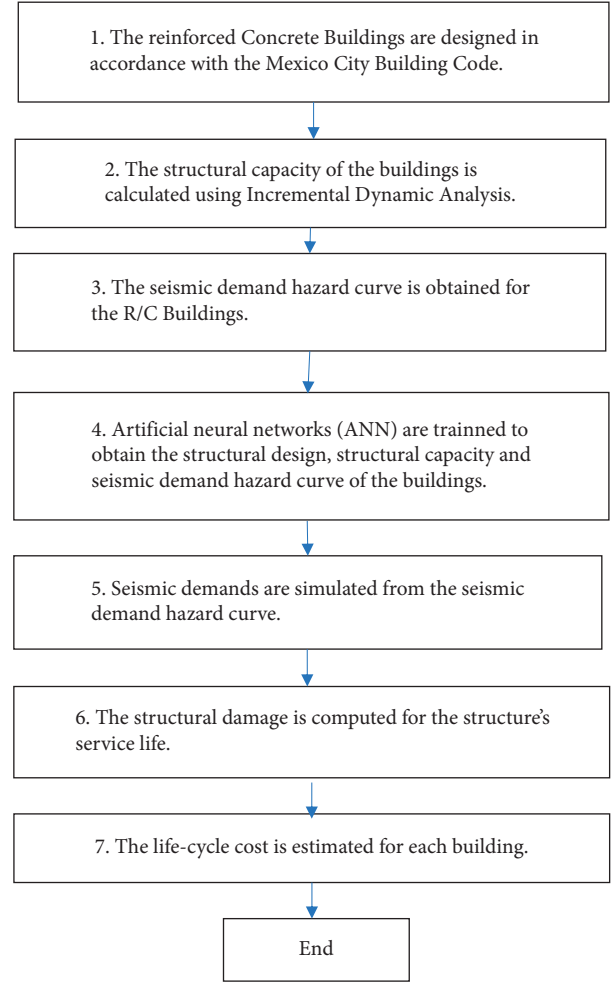


FIGURE 1: Flowchart of the life-cycle cost assessment procedure.

**2.3. Structural Reliability (Step 3).** The structural reliability is obtained from the seismic demand hazard curve that estimates the mean of the annual rate of exceeding a certain MID. The curve is calculated by the following expression [33,34]:

$$\left| \frac{d\nu(S_a)}{d(S_a)} \right| P(D > d | S_a) d(S_a), \quad (1)$$

Where  $\nu_D(d)$ : represents the average number of times per year that MID exceed a given value of  $d$ ;  $d$ : a given value of MID;  $D$ : structural demand, presented by the maximum inter-story drift;  $S_a$ : pseudo-acceleration associated with the fundamental period of vibration of the building;  $\nu(S_a)$ : the seismic hazard curve for the site of interest; and

$$P(D > d | S_a) = 1 - \Phi\left(\frac{\ln(D) - \hat{\mu}_{\ln d}}{\hat{\sigma}_{\ln d}}\right), \quad (2)$$

where  $P(D > d | S_a)$ : is the fragility curve;  $\Phi$ : the standard normal cumulative distribution function;  $\hat{\mu}_{\ln d}$ : the median of the logarithmic value of the seismic demand;  $\hat{\sigma}_{\ln d}$ : logarithmic standard deviation of the demand.

**2.4. Artificial Neural Network Training (Step 4).** In this study, the artificial neural network technique has been used for the structural design of the buildings and to estimate the capacity and seismic demand hazard curves. From the previous steps, and in order to obtain the structural capacity and seismic demand hazard curve, numerous nonlinear analyses that are time consuming are required. Therefore, it is possible to reduce the time for the analysis of the building using ANN models. The Matlab [35] software was used in this study to develop the ANNs.

**2.5. Seismic Demands Simulation (Step 5).** Different values of seismic demands are simulated from the seismic demand hazard curve (equation (1)). For the numerical simulation, the average number of times per year that a seismic event occurs with a magnitude equal or greater than 6 is considered  $\nu = 3$ . The events are modeled by a Poisson process; therefore, the earthquakes follow an exponential distribution. By using the inverse transformation method [36] different values of MID are simulated for the life-cycle of the buildings.

**2.6. Damage Index (Step 6).** There are different approaches to estimate the structural damage [37,38]. In the present study, the level of structural degradation is estimated from a measure of physical damage, which is represented as a damage index, DI, expressed as the ratio between the global structural capacity of the building and structural demand. The values taken by the DI are between 0 and 1, when DI equals 0 represents no damage in the structure, and DI equals 1 represents the total damage. The DI is defined by equation (3) [39]:

$$DI = \frac{\delta_D - \delta_y}{\delta_u - \delta_y}, \quad (3)$$

Where  $\delta_D$ : is the maximum inter-story drift demand, which is obtained from the simulation of the seismic demands of the seismic demand hazard curve (step 5);  $\delta_y$ : is the maximum inter-story drift associated with serviceability limit state (structure without damage), which is obtained from the statistic value of the limit state considered in the incremental dynamic analyses;  $\delta_u$ : is the maximum inter-story drift associated with incipient collapse.

**2.7. Life Cycle Cost Functions (Step 7).** The total cost of a structure with an expected life cycle of 50 years is the combination of the initial cost plus the expected damage cost:

$$C_t = C_I + C_D, \quad (4)$$

Where  $C_t$ : represents the total cost of the structure;  $C_I$ : is the initial cost;  $C_D$ : is the cost associated with the damage.

**2.7.1. Initial Cost.** The initial cost is calculated using an approximated procedure proposed by De Leon [14]. The cost includes direct cost, indirect costs and the utility paid

to the contractor. The direct cost  $C_{DI}$  is estimated from the material cost  $C_M$  plus the cost of labor, approximately 40% of  $C_M$ ,  $C_{DI} = 1.4C_M$ . The indirect cost due to the nonstructural work the contractor has (i.e.: insurance, training, office expenses, etc.) is estimated to be 20% of  $C_{DI}$ ,  $C_{IN} = 0.2C_{DI}$ . The constructor fee is 15% of the summation of the direct cost and indirect cost,  $U_M = 0.15(C_{DI} + C_{IN})$ . The total initial cost can be estimated as the summation of  $C_{DI}$ ,  $C_{IN}$  and  $U_M$ , equation (5);

$$C_I = C_{DI} + C_{IN} + U_M = 1.38C_{DI} = 1.93C_M. \quad (5)$$

Where;  $C_I$ : is the initial cost;  $C_{DI}$ : is the direct cost;  $C_{IN}$ : is the indirect cost;  $U_M$ : is the utility.

The unit cost of the construction materials  $C_M$  is shown in Table 1. For the cost analyses the average cost of concrete and steel in Mexico City is used.

**2.7.2. Damage Cost.** The damage costs  $C_D$  of the structure during its useful life can be express as the following: repair or reconstruction,  $C_{PR}$ ; loss of content,  $C_{PC}$ ; economic losses,  $C_{PI}$ ; injury,  $C_{PL}$ ; and loss of life,  $C_{PV}$ . The damage cost can be expressed as Eq. (6);

$$C_d = C_{PR} + C_{PC} + C_{PI} + C_{PL} + C_{PV}. \quad (6)$$

The damage costs are obtained by means of the simulated level of structural damage present in the building. The damage index (Step 6) is used to measure the structural damage simulated.

**(1) Repair Cost or Reconstruction.** There are several methods to repair buildings damaged by previous earthquakes, depending on factors such as the level of damage, type of structure, configuration, logistics. In this study, it is assumed that the R/C buildings will be repaired using the jacketing technique of structural members, this technique allows the structure to be repaired effectively and return to practically its initial condition before the damage. Based on the repair costs of buildings that were damaged by previous earthquakes a relationship between the repair cost and the damage index was established. The structural damage in some cases is extremely severe such structures can no longer be repaired, and it is necessary to be demolished. De León and Ang [40] considered that for  $DI > 0.70$  the R/C structure needs to be demolished. The costs of reconstruction are assumed to be equal to  $1.2 C_I$ , which includes costs of demolition, cleaning and redesigning the structure. For  $DI < 0.70$  the repair cost is a function of the initial cost times the DI to the second power. The repair or reconstruction costs are defined by equation (7) and (8):

$$C_{PR} = (C_I)DI^2, \quad 0 \leq DI < 0.7, \quad (7)$$

$$C_{PR} = 1.2C_I, \quad DI \geq 0.7. \quad (8)$$

The relationship between the normalize repair cost ( $C_{PR}/C_I$ ) and the damage index is shown in Figure 2.

TABLE 1: Unitary cost of materials.

| Material                                 | Cost (\$US Dollar)   |
|--|----------------------|
| Steel                                    | \$1000/ton           |
| Concrete ( $f_c = 250 \text{ kg/cm}^2$ ) | \$130/m <sup>3</sup> |

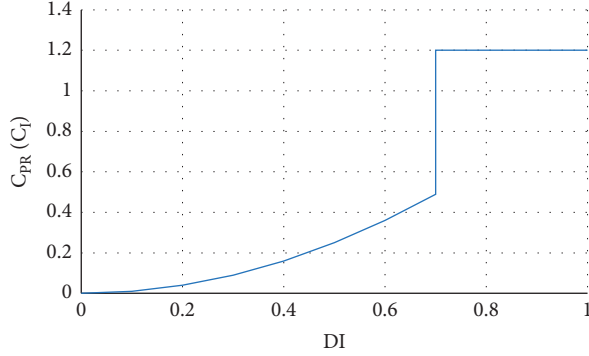


FIGURE 2: Repair cost as function of damage index.

(2) *Cost Due to Damage of Contents.* The estimation of costs due to damage of contents depends on the type and use of the structure; for example, the damage of contents in a school does not have the same impact as that of an office building or shopping mall. In this study, it is assumed that the buildings are offices, it is considered as suggested by Suranhman and Rojiani [41], that the maximum content loss if  $DI > 1$  is equal to 50% of the initial cost. For values of  $DI < 1$ , the expected cost is assumed to be a linear function of  $DI$ . The cost due to loss of content is defined by equations (9) and (10):

$$C_{PC} = 0.5(C_I)DI, \quad 0 < DI < 1.0. \quad (9)$$

$$C_{PC} = 0.5C_I, \quad DI \geq 1.0. \quad (10)$$

The relationship between the normalized cost due to damage of contents ( $C_{PR}/C_I$ ) and the damage index is shown in Figure 3.

(3) *Cost Due to Economic Loss.* The cost due to economic loss depends on the economic activity for which the building is used. This study assumed the usage of the building as offices; therefore, the economic loss is associated with the loss of income due to rental during the time of repair or reconstruction.

The maximum cost for economic loss ( $DI > 1$ ) is a function of the period of reconstruction ( $P_R$ ), the average rent in dollars per square meter ( $R$ ) and the build area in meters of the structure ( $A$ ). For values of  $DI < 1$  the variation of cost is assumed to be a function of  $DI$  to the second power [14]. The average monthly rental for offices in Mexico City is equal to \$19 US dollars/m<sup>2</sup> and it is assumed that the maximum period of reconstruction of a building is equal to 24 months. The function due to economic loss is defined by equations (11) and (12).

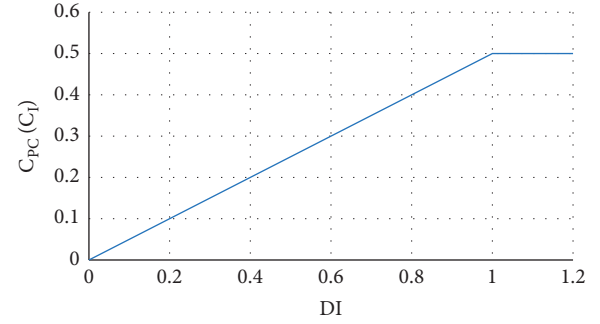


FIGURE 3: Loss of content cost as function of damage index.

$$C_{PI} = R(P_R)A, \quad DI \geq 1. \quad (11)$$

$$C_{PI} = R(P_R)(A)DI^2, \quad 0 < DI < 1.0. \quad (12)$$

The relationship between the normalized economic cost per square meter of building area ( $C_{PI}/A$ ) and the damage index is shown in Figure 4.

(4) *Cost Due to Loss of Life.* The estimation of the cost associated with life loss is a difficult task because it is a sensitive issue [42–45]. Two postures regarding the value of a person life can be found. The first one, human life has a statistical value based on its income; and the second one, the cost of human life is invaluable. For this work, the value of a life is considered by the average income of a person.

For the present study, the cost due to the loss of life is estimated relying on previous catastrophic seismic events. For this reason, it is necessary to estimate the average number of dead people inside a building during a seismic event. A nonlinear regression analysis [40] was obtained based on the total area of buildings that collapse during the 1985 Mexico City earthquake [46] and the number of deaths [47]. The result of this analysis is summarized in equation (13) and shown in Figure 5:

$$N_d = 45.48 + 5.531744A^2. \quad (13)$$

Where  $N_D$ : is the number of deaths;  $A$ : is the of collapsed buildings area in 1000 m<sup>2</sup>.

The cost due to the loss of life function ( $DI > 1$ ) is expressed as the total number of deaths,  $N_D$ , in the case of incipient collapse, multiplied by the value of the statistical life-time income of a person,  $C_{PF}$ . For smaller vales of  $DI$ , it is assumed that the cost function can be represented by the total number of deaths, multiplied by the statistical life-time income of a person multiplied by  $DI$  to the fourth power, Equation (15). It is considered that the average annual income of a person in Mexico is considered equal to \$10000 US dollars [48], and that the useful working life per person is equal to 25 years, so the cost per death ( $C_{PF}$ ) of a person is equal to \$250,000 US dollars. The cost functions due to loss of life are summarized in equations (14) and (15) [14]:

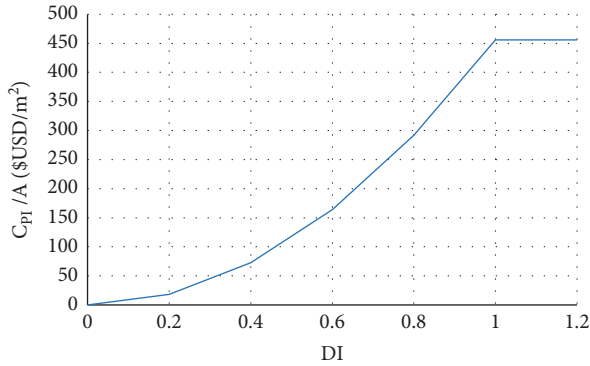


FIGURE 4: Economic loss as function of the damage index.

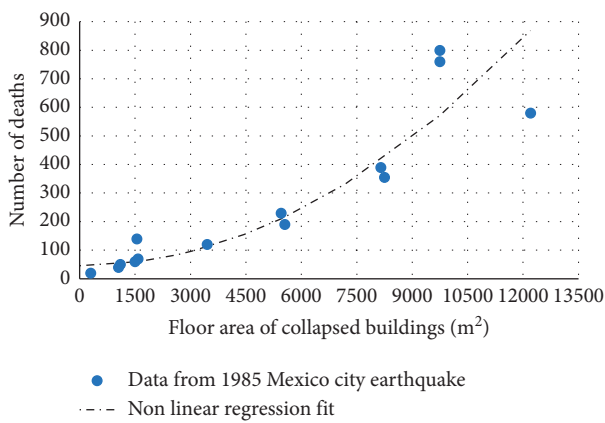


FIGURE 5: Number of deaths vs area of collapsed buildings.

$$C_{PV} = N_D (C_{PF} DI^4), \quad 0 < DI < 1. \quad (14)$$

$$C_{PV} = N_D C_{PF}, \quad DI \geq 1. \quad (15)$$

(5) *Cost Due to Injuries.* The evaluation of cost due to injuries,  $C_{PL}$ , refers to expenses required for hospitalization of people who became injured during an earthquake [14]. The average number of people injured per unit area of collapse is equal to  $0.0168/\text{m}^2$  estimated as the relation of the number of injuries reported in the 1985 Mexico City earthquake [47] with the total area of buildings collapsed [46]. The cost of injuries without disability,  $C_{LS}$ , is considered equal to \$2000 US dollars. Notice that costs for minor injuries, medical expenses and medicine, including a small stay in the hospital are considered. Injured without disability are considered to represent 90% of all injured people [40]. The cost of injuries resulting in disability,  $C_{LI}$ , is considered equal to \$250,000 US dollars (equal to the cost of death). People with disabilities represent 10% of total injuries.

For  $DI < 1$  the cost due to injuries is assumed to be a function of the total people injured in the building times the DI raised to the second power, Equation (16) [14]. For  $DI > 1$  the cost function is assumed to be a function of the total people injured in the building with disability and without disability in the building, Equation (17).

$$C_{PL} = (0.1C_{LI} + 0.9C_{LS})0.0168(A)DI^2, \quad 0 < DI < 1, \quad (16)$$

$$C_{PL} = (0.1C_{LI} + 0.9C_{LS})0.0168A, \quad DI \geq 1. \quad (17)$$

The relationship between the normalized cost due to injuries per person injured ( $C_{PL}$ ) and the damage index is shown in Figure 6.

### 3. Illustrative Example

The illustration of the methodology is presented by an example in this section. The methodology is applied to a 12-story, 3-bays reinforced concrete building.

*3.1. Selected Ground Motion Records.* In this study three different buildings are located in soft soil with a dominant period  $T_S = 2.0\text{s}$ . A set of 15 ground motion records were selected to perform the analyses of the buildings. Table 2 shows the main characteristics of the earthquake ground motions. The ground motion records were obtained from the IINGEN database [49]. The pseudo-acceleration elastic seismic response spectra of the records selected are shown in Figure 7 considering 5% of critical damping.

Figure 8 shows the seismic hazard curves associated with different fundamental structural periods. Those curves represent the probability that a structure will exceed a specified seismic intensity (e.g., pseudo-acceleration) in one year. The curves are used to solve Eq. 1, and corresponds to a site located at soft soil of Mexico City.

*3.2. Reinforced Concrete Building Characteristics.* Three types of reinforced concrete buildings, low, mid, and high rise were selected for the seismic analyses and design according with common practice in Mexico City. The buildings were represented by three-dimensional structural models with elevation between 4, 8, and 12 stories, an inter-story height equal to 4 meters. The buildings are constituted by orthogonal rigid reinforced concrete frames constituted by beams and columns, with three bays in both directions. While for the 4-story building the bay length is equal to 6m, for the 8 and 12-story buildings the bay length is equal to 8m. The frames are connected by floor slabs assumed to be rigid diaphragms. Figure 9 shows the geometric characteristics of the buildings.

*3.3. Structural Design.* The 12-story building is designed in accordance with the Mexico City Building Code [50]. The loads considered for the analysis are; dead load, live load and seismic load.

The 12-story building was divided into 3 groups of beams and 3 groups of columns to uniform the buildings sections. Table 3 shows the results of the structural design for the 12-story building. The sections characteristics shown in Table 3 are the parameters for beams; b: width, h: depth,  $A_{se}$ : longitudinal reinforcement inferior at the end region of beam,  $A_{se}'$ : longitudinal reinforcement superior at the end region of beam,  $A_{sm}$ : longitudinal reinforcement inferior at

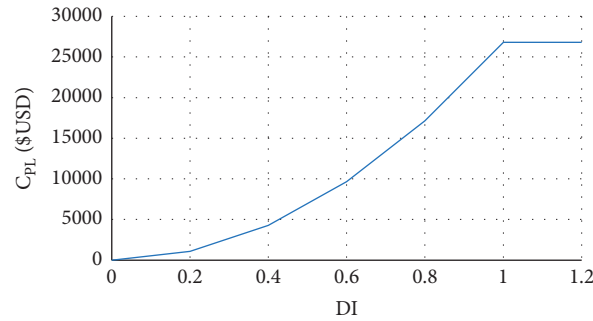


FIGURE 6: Cost of Injuries per person as a function of the damage index.

TABLE 2: Earthquake ground motions recorded on soft soil  $T_s = 2.0s$  in Mexico City.

| EQ. | Date     | Epicenter Coordinates | Magnitude | Station | Location  |
|-----|----------|-----------------------|-----------|---------|---|
| S1  | 97-01-11 | 18.220 N; 102.76 W    | 6.9       | RIDA    | RED INTERUNIVERSITARIA DE INSTRUMENTACION SISIMICA (RIIS) |
| S2  | 89-04-25 | 16.603 N; 99.400 W    | 6.9       | DR16    | CENTRO DE INSTRUMENTACION Y REGISTRO SISMICO (CIRES)      |
| S3  | 97-01-11 | 17.9 N; 103.0 W       | 6.9       | DR16    | CENTRO DE INSTRUMENTACION Y REGISTRO SISMICO (CIRES)      |
| S4  | 95-09-14 | 16.31 N; 98.88 W      | 7.3       | IMPS    | CENTRO NACIONAL DE PREVENCION DE DESASTRES (CENAPRED)     |
| S5  | 97-01-11 | 18.09 N; 102.86 W     | 6.9       | IMPS    | CENTRO NACIONAL DE PREVENCION DE DESASTRES (CENAPRED)     |
| S6  | 95-09-14 | 18.02 N; 101.56 W     | 7.3       | CHAS    | CENTRO NACIONAL DE PREVENCION DE DESASTRES (CENAPRED)     |
| S7  | 89-04-25 | 16.603 N; 99.400 W    | 6.9       | EO30    | CENTRO DE INSTRUMENTACION Y REGISTRO SISMICO (CIRES)      |
| S8  | 89-04-25 | 16.603 N; 99.400 W    | 6.9       | CO47    | CENTRO DE INSTRUMENTACION Y REGISTRO SISMICO (CIRES)      |
| S9  | 95-09-14 | 16.31 N; 98.88 W      | 7.3       | CO47    | CENTRO DE INSTRUMENTACION Y REGISTRO SISMICO (CIRES)      |
| S10 | 81-10-25 | 17.880 N; 102.150 W   | 7.3       | SXVI    | INSTITUTO DE INGENIERÍA. UNAM                             |
| S11 | 85-09-19 | 18.081 N; 102.942 W   | 8.1       | SXVI    | INSTITUTO DE INGENIERÍA. UNAM                             |
| S12 | 95-09-14 | 16.31 N; 98.88 W      | 7.3       | COYS    | CENTRO NACIONAL DE PREVENCION DE DESASTRES (CENAPRED)     |
| S13 | 95-09-14 | 16.31 N; 98.88 W      | 7.3       | PII6    | CENTRO DE INSTRUMENTACION Y REGISTRO SISMICO (CIRES)      |
| S14 | 95-09-14 | 16.31 N; 98.88 W      | 7.3       | FJ74    | CENTRO DE INSTRUMENTACION Y REGISTRO SISMICO (CIRES)      |
| S15 | 95-09-14 | 16.31 N; 98.88 W      | 7.3       | CS78    | CENTRO DE INSTRUMENTACION Y REGISTRO SISMICO (CIRES)      |

the mid span,  $As_m$ : longitudinal reinforcement superior at the mid span,  $s_e$ : stirrups spacing at the end of the beam,  $s_m$ : stirrups spacing in the middle of the beam, for columns;  $b$ : width,  $h$ : depth,  $A_s$ : longitudinal reinforcement,  $s$ : stirrups spacing.

**3.4. Building Structural Capacity.** The structural capacity of the building is calculated using incremental dynamic analysis. For this aim, the software Ruaumoko3D [51] was used to apply a series of nonlinear structural analyses to the building in order to determine the structural behavior.

Nonlinear structural analysis is performed by subjecting the structure to a set of records (Table 2) scaled at different increasing levels of pseudo-acceleration. The result extracted from each analysis is a discrete point used to form the IDA curve (see Figure 10). The modified Takeda hysteretic model was considered in the analyses to assume the degradation of stiffness and strength of the reinforced concrete elements.

The limit state near collapse is defined within the Ruaumoko computer program when one of the following conditions are reached: (a) Numerical instability, (b) decrement of the tangent lateral stiffness to 20% of the initial value or, c) ultimate rotation condition of a member. The

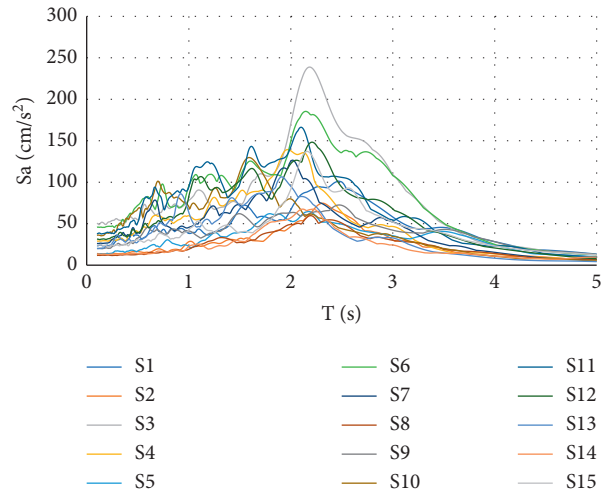


FIGURE 7: Seismic response spectra of the selected ground motions for soft soil with  $T_s = 2.0$ .

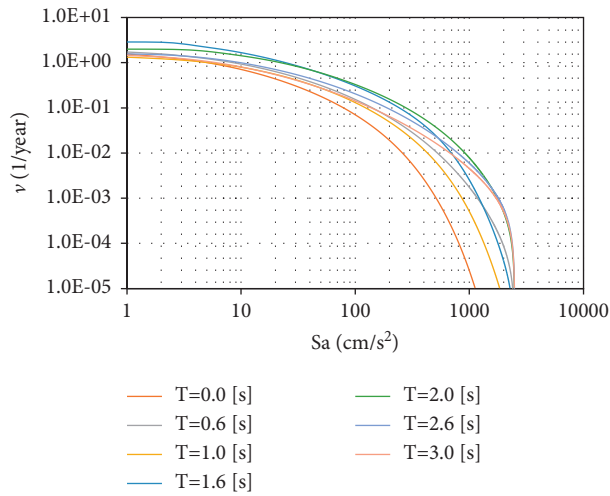


FIGURE 8: Seismic hazard curves.

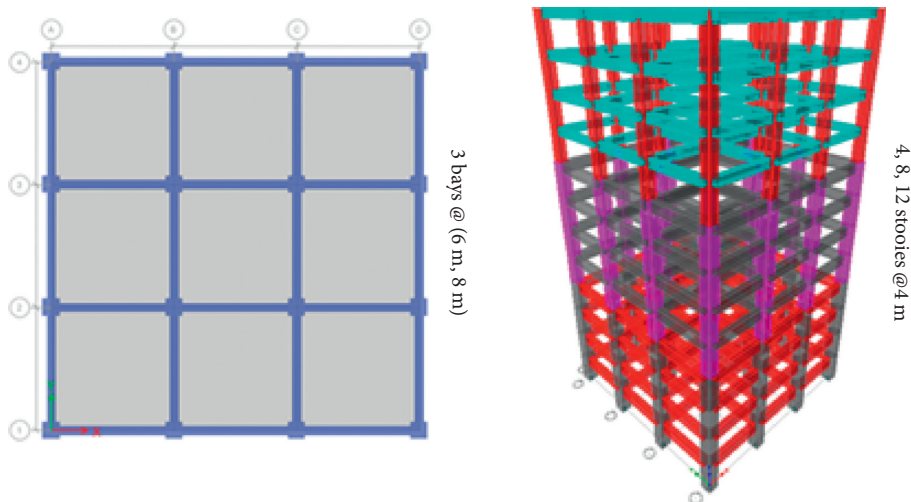


FIGURE 9: Plan and elevation of the reinforced concrete buildings.

TABLE 3: 12-story building structural design.

| Parameter | Units | Parameter       | Units |        |                 |
|-----------|-------|-----------------|-------|--------|-----------------|
| b         | 70    | cm              | Ase   | 41.10  | cm <sup>2</sup> |
| h         | 150   | cm              | Ase'  | 29.57  | cm <sup>2</sup> |
| Ase       | 72.21 | cm <sup>2</sup> | Asm   | 11.19  | cm <sup>2</sup> |
| Ase'      | 59.77 | cm <sup>2</sup> | Asm'  | 15.43  | cm <sup>2</sup> |
| Asm       | 26.66 | cm <sup>2</sup> | se    | 6      | cm              |
| Asm'      | 27.46 | cm <sup>2</sup> | sm    | 7      | cm              |
| se        | 4     | cm              | b     | 130    | cm              |
| sm        | 4     | cm              | h     | 130    | cm              |
| b         | 65    | cm              | As    | 471.78 | cm <sup>2</sup> |
| h         | 130   | cm              | s     | 3      | cm              |
| Ase       | 63.99 | cm <sup>2</sup> | b     | 130    | cm              |
| Ase'      | 53.58 | cm <sup>2</sup> | h     | 130    | cm              |
| Asm       | 21.32 | cm <sup>2</sup> | As    | 286.55 | cm <sup>2</sup> |
| Asm'      | 24.56 | cm <sup>2</sup> | s     | 3      | cm              |
| se        | 4     | cm              | b     | 110    | cm              |
| sm        | 4     | cm              | h     | 110    | cm              |
| b         | 45    | cm              | As    | 234.83 | cm <sup>2</sup> |
| h         | 100   | cm              | s     | 5      | cm              |

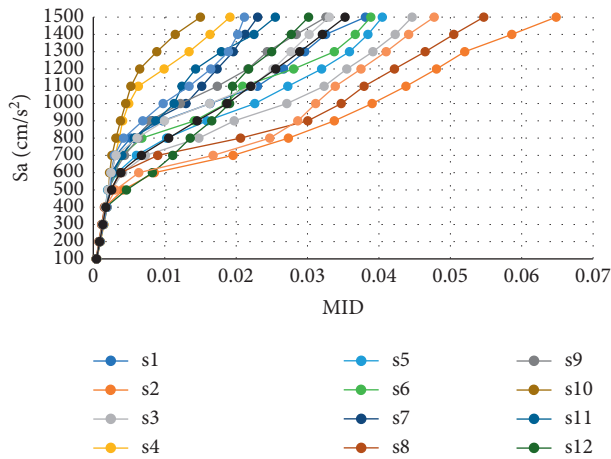


FIGURE 10: IDA curves for 12-story building.

yielding limit state was defined as the difference of 10% of the elastic slope.

**3.5. Seismic Demand Hazard Curve.** In order to obtain the seismic demand hazard curves, the fragility curves for the 12-story building are needed. The fragility curves represent the conditional probability of damage being exceeded a particular damage state, these curves are obtained from Eq. 2.

Figure 11 presents a set of 12 fragility curves. Those curves show the vulnerability of the building underground motions, it represents the conditional probability of exceeding a maximum inter-story drift ( $d$ ) as stated in the Mexico City Building Code [50]. Two limit states are considered, the service limit state and near collapse state. This figure illustrates that when a ground motion intensity  $S_a = 900 \text{ cm/s}^2$ , the probability of reaching or exceeding  $d = 0.015$  is approximately 30% for the 12-story building.

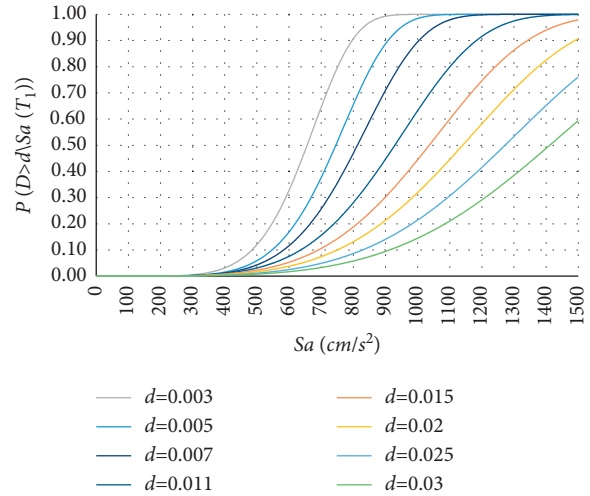


FIGURE 11: Fragility curves for the 12-story building.

From the figure it can be seen that for the same intensity  $S_a$ , the exceedance probability ( $P$ ) decreases as the peak inter-story drift ( $d$ ) value increases. The seismic demand hazard curve show in Figure 12 was obtained from Eq. 1, and it represents the mean annual rate of exceeding a maximum inter-story drift ( $d$ ).

**3.6. Reliability Analysis Using Artificial Neural Networks.** In this study, the technique of artificial neural networks is used, first; to design buildings based on similar characteristics of the buildings used in the database, second; to estimate the structural capacity and the seismic demand hazard curve. Two different ANN models were trained using data from a set of buildings designed in previous studies [52–54].

For the training phase of the first model a feedforward backpropagation network was used to design a 12-story building. The architectural model of the ANN used was an input layer, hidden layers and the output layer, with 7 neurons for the input layer, 5 neurons for the hidden layer and 36 neurons for the output. The activation functions were hyperbolic tangent sigmoid (tansig) for the hidden and output layer. A set of 200 buildings were used as data for the training phase of the first ANN model. The 7 neurons in the input layer represents the general characteristics of the buildings; number of bays in  $X$  direction, number of bays in  $Y$  direction, story levels, story height, bays spacing  $X$ , bays spacing  $Y$ , soil period. The 36 output neurons represent the parameters of the beams and columns designed.

The results of the design obtained from the first ANN model are shown in Table 4, which are compared with the results obtained using traditional approaches for seismic design (see Table 3). The results showed excellent similarity with the actual values, attaining a good accuracy prediction with a relative error less than 9%. Moreover, the selected 12-story building was not used in the dataset of the training phase.

The second ANN model estimates the seismic demand hazard curve and capacity of the 12-story building. The input

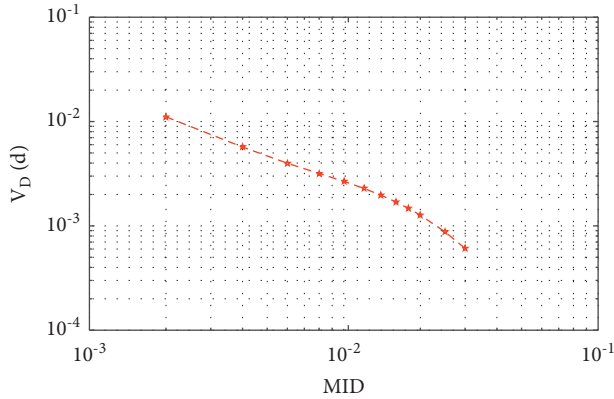


FIGURE 12: Seismic demand hazard curve.

TABLE 4: 12-story building structural design using ANN.

| Parameter | Units  | Parameter       | Units |        |                 |
|-----------|--------|-----------------|-------|--------|-----------------|
| b         | 72.90  | cm              | Ase   | 38.72  | cm <sup>2</sup> |
| h         | 155.27 | cm              | Ase'  | 24.60  | cm <sup>2</sup> |
| Ase       | 70.73  | cm <sup>2</sup> | Asm   | 9.79   | cm <sup>2</sup> |
| Ase'      | 58.54  | cm <sup>2</sup> | Asm'  | 13.93  | cm <sup>2</sup> |
| Asm       | 27.85  | cm <sup>2</sup> | se    | 6.7    | Cm              |
| Asm'      | 28.54  | cm <sup>2</sup> | sm    | 9.5    | Cm              |
| se        | 3.7    | cm              | b     | 137.37 | Cm              |
| sm        | 3.6    | cm              | h     | 137.37 | Cm              |
| b         | 65.31  | cm              | As    | 492.75 | cm <sup>2</sup> |
| h         | 138.69 | cm              | s     | 2.4    | cm              |
| Ase       | 62.82  | cm <sup>2</sup> | b     | 130.62 | cm              |
| Ase'      | 50.92  | cm <sup>2</sup> | h     | 130.62 | cm              |
| Asm       | 22.24  | cm <sup>2</sup> | As    | 286.10 | cm <sup>2</sup> |
| Asm'      | 23.74  | cm <sup>2</sup> | s     | 3.2    | cm              |
| se        | 4.2    | cm              | b     | 106.76 | cm              |
| sm        | 4.2    | cm              | h     | 106.76 | cm              |
| b         | 43.24  | cm              | As    | 283.24 | cm <sup>2</sup> |
| h         | 90.53  | cm              | s     | 5.6    | cm              |

layer with 44 neurons, two hidden layers with 5 neurons and the output layer with 14 neurons, constitutes the architectural model used in the second ANN tool. The same set of 200 buildings was used in the training phase. The activation functions were hyperbolic tangent sigmoid (tansig) for the two hidden layers, and output layer. The input layer parameters are the buildings general and section characteristics and the output layer represents the capacity and seismic demand hazard curve. Table 5 summarizes the input vector parameters.

Figure 13 shows the results of the ANN model and the comparison to those obtained using equation (1). From the figure, it can be seen that the estimation of the seismic demand hazard curve simulated with the ANN; SIM curve, attained good accuracy on predicting equation (1), with a mean square error (MSE) of 2.42e-08 about 9% relative error.

3.7. Seismic Demand Simulation. The simulation of the seismic demands considering 50 years of service life is

TABLE 5: Input vector of the second ANN model.

| Input parameter            | Units           | Input parameter | Units           |
|----------------------------|-----------------|-----------------|-----------------|
| Number of bays X direction |                 | b               | cm              |
| Number of bays Y direction |                 | h               | cm              |
| STory levels               |                 | Ase             | cm <sup>2</sup> |
| Bays spacing X             |                 | Ase'            | cm <sup>2</sup> |
| Bays spacing Y             |                 | Asm             | cm <sup>2</sup> |
| Dead load design factor    |                 | Asm'            | cm <sup>2</sup> |
| Live load design factor    |                 | se              | cm              |
| Seismic load design factor |                 | sm              | cm              |
| b                          | cm              | b               | cm              |
| h                          | cm              | h               | cm              |
| Ase                        | cm <sup>2</sup> | As              | cm <sup>2</sup> |
| Ase'                       | cm <sup>2</sup> | s               | cm              |
| Asm                        | cm <sup>2</sup> | b               | cm              |
| Asm'                       | cm <sup>2</sup> | h               | cm              |
| se                         | cm              | As              | cm <sup>2</sup> |
| sm                         | cm              | s               | cm              |
| b                          | cm              | b               | cm              |
| h                          | cm              | h               | cm              |
| Ase                        | cm <sup>2</sup> | As              | cm <sup>2</sup> |
| Ase'                       | cm <sup>2</sup> | s               | cm              |
| Asm                        | cm <sup>2</sup> |                 |                 |
| Asm'                       | cm <sup>2</sup> |                 |                 |
| se                         | cm              |                 |                 |
| sm                         | cm              |                 |                 |

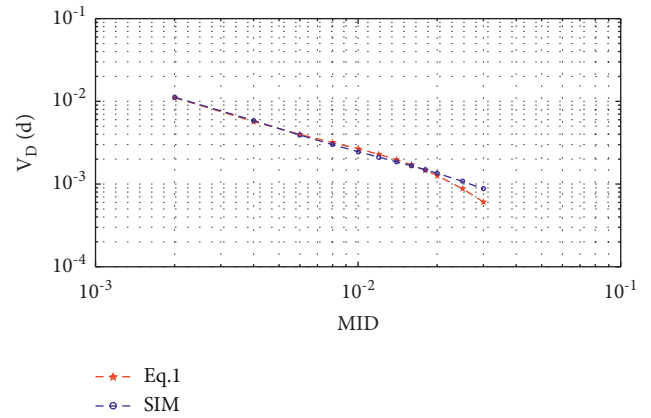


FIGURE 13: 12-story building seismic demand hazard curve results comparison using equation (1) and the ANN model.

performed using the seismic demand hazard curve estimated by the ANN. For the simulation, the average number of seismic events per year is needed, in this study an average number of 3 seismic events with magnitude equal or greater than 6 was used [22]. Figure 14 shows the seismic demands in terms of MID, considering the service life for the 12-story building.

3.8. Damage Index in Service Life of the Building. The damages are evaluated using equation (3). The damage index is then obtained for every seismic demand simulated for the service life of the building. The limit state associated with serviceability,  $\delta_y = 0.0018$ , and the limit state associated

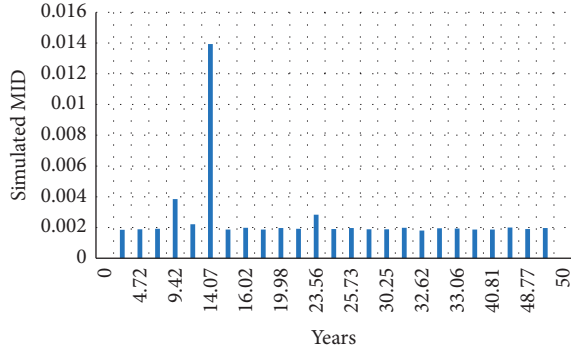


FIGURE 14: Simulated maximum inter-story drift.

with incipient collapse,  $\delta_u = 0.0356$ , were obtained from the results of the ANN training. Figure 15 shows the damage index for the simulated demands scenario of Figure 14.

**3.9. Cost of the 12 Story Building.** The initial cost of the 12-story building is obtained from the amount of material (concrete and steel) necessary for its construction. The material is obtained from the quantification of the material necessary to build the beam and column elements obtained from the structural design, 557 tons of reinforced steel and 3660 cubic meters of concrete were quantified. Equation (5) is applied to obtain the initial costs.

$$C_I = 1.93 * ((557 * 1000) + (3660 * 130)) = \quad (18)$$

The damage costs are obtained for the simulated seismic demand of the year 14.07, where the demand is 0.014 for the 12-story building. Applying equation (3) for the year 14.07, the damage index is 0.359 (Figure 15). The costs due to damage are then:

Repair cost or reconstruction (Equation (7)):

$$C_{PR} = (1.993)(0.359)^2 = 0.256 \text{ MM}. \quad (19)$$

Cost due to damage of contents (Equation (9)):

$$C_{PC} = 0.5(1.993)(0.359) = 0.357 \text{ MM}. \quad (20)$$

Cost due to economic loss (Equation (12)):

$$C_{PI} = 19(24)(6912)(0.359)^2 = 0.406 \text{ MM}. \quad (21)$$

Cost due to loss of life (Equations (13) and (14)):

$$N_d = 45.48 + 5.531744(6.912)^2 = 310N_d, \quad (23)$$

$$C_{PV} = 310(250000)(0.359)^4 = \$1.289 \text{ MM}.$$

Cost due to injuries (Equation (16))

$$C_{PL} = (0.1(250000) + 0.9(2000))0.0168(6912)(0.359)^2 = \$0.401 \text{ MM}. \quad (24)$$

The total costs due to damage for the year 14.07 was obtained by the summation of all the costs due to damage (Equation (6)).

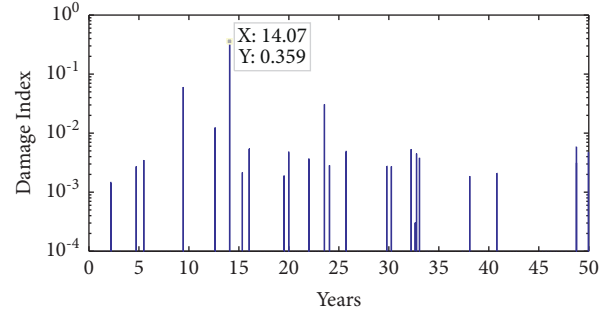


FIGURE 15: Damage index scenario for the service life of the 12-story building.

$$C_d = 0.256 + 0.357 + 0.406 + 1.289 + 0.401 = \$2.709 \text{ MM}. \quad (25)$$

## 4. Results and Discussion

This section shows the results of applying the methodology for the 4, 8 and 12 story buildings.

The ANN prediction results of the seismic demand hazard curve are compared to those of Equation (1). Figure 16 shows the predicted values of the seismic demand hazard curve for the 4-story building (SIM curve), based on the results of the predictions done by the ANN, the curve shows a deviation from the curve of Eq.1. The mean square error  $2.97e-07$  is estimated from the deviation, about a 12% of relative error; therefore, the usefulness of the seismic demand hazard curve to simulate the seismic demand during the life-cycle of the building is sufficient to predict accurate demand values. The seismic demand hazard curve for the 8-story building is shown in Figure 17, where the mean square error estimated from the deviation of the curve predicted by the ANN is  $3.81Ee-07$ , about a 6% of relative error.

The initial cost of the 4-story building is obtained by applying Equation (5). The amount of material necessary for the construction was obtained from the quantification of the material necessary to build the structural members given by the structural design of the ANN, a total of 39.5 tons of steel and 353.75 cubic meters of concrete were obtained. By applying Equation (5) and multiplying by unit cost of the material (Table 1) the initial cost  $C_I =$  US dollars.

Table 6 shows the cost due to damage expected over the life cycle of the 4-story building. From the table it can be seen the damage scenario simulated throughout the 50 year life-cycle of the building, and the damage cost associated with that damage. The total life-cycle cost for the 4-story building is the sum of the initial cost plus the cost due to damage  $C_t = 164,991$  US dollars.

To estimate the initial cost for the 8-story building, the ANN was used to design the building and quantify the material necessary for its construction. A total of 230 tons of steel and 1905 cubic meters of concrete were quantified. The initial cost is obtained applying equation (5), the cost is  $C_I =$  US dollars. The damage cost for the simulated structural

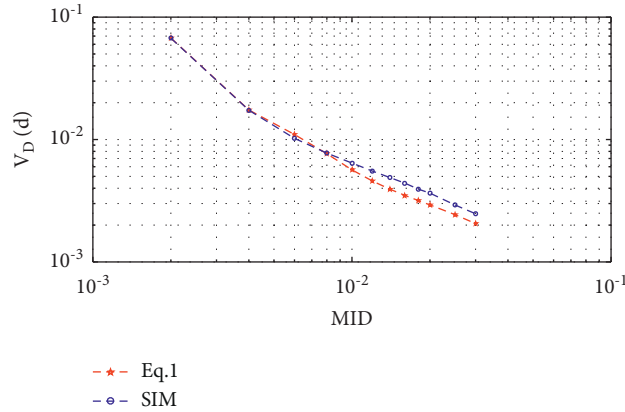


FIGURE 16: 4-story building seismic demand hazard curve results comparison using Equation (1) and ANN model.

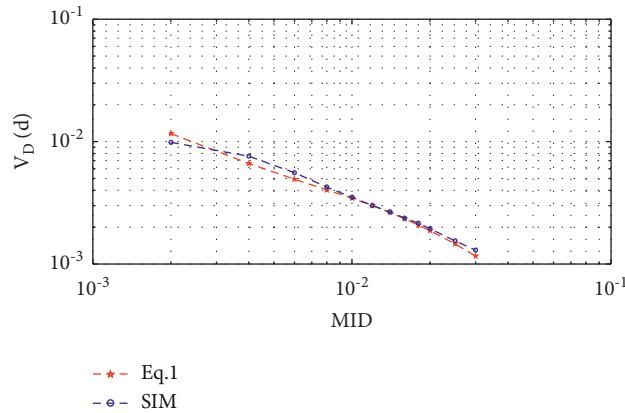


FIGURE 17: 8-story building seismic demand hazard curve results comparison using Equation (1) and ANN model.

TABLE 6: Expected damage cost in the life-cycle of the 4-story building.

| Year  | DI     | C <sub>PR</sub> | C <sub>PC</sub> | C <sub>PI</sub> | C <sub>PL</sub> | C <sub>PV</sub>   | C <sub>d</sub>   |
|-------|--------|-----------------|-----------------|-----------------|-----------------|-------------------|------------------|
| 0.97  | 0.0060 | \$5.91          | \$493.90        | \$21.18         | \$0.02          | \$20.92           | \$541.93         |
| 1.75  | 0.1147 | \$2,171.08      | \$9,463.19      | \$7,776.51      | \$2,350.17      | \$7,678.28        | \$29,439.23      |
| 5.75  | 0.0110 | \$19.92         | \$906.44        | \$71.35         | \$0.20          | \$70.45           | \$1,068.35       |
| 11.47 | 0.0365 | \$220.10        | \$3,013.05      | \$788.35        | \$24.15         | \$778.40          | \$4,824.04       |
| 17.48 | 0.0095 | \$14.93         | \$784.82        | \$53.49         | \$0.11          | \$52.81           | \$906.17         |
| 31.81 | 0.0074 | \$9.02          | \$609.84        | \$32.30         | \$0.04          | \$31.89           | \$683.08         |
| 37.28 | 0.0017 | \$0.46          | \$137.99        | \$1.65          | \$0.00          | \$1.63            | \$141.74         |
| 39.73 | 0.0275 | \$125.16        | \$2,272.15      | \$448.32        | \$7.81          | \$442.65          | \$3,296.09       |
| 41.52 | 0.0002 | \$0.01          | \$14.57         | \$0.02          | \$0.00          | \$0.02            | \$14.61          |
| 45.87 | 0.0198 | \$64.81         | \$1,634.99      | \$232.13        | \$2.09          | \$229.20          | \$2,163.23       |
| 45.99 | 0.2157 | \$7,677.55      | \$17,795.54     | \$27,499.99     | \$29,389.64     | \$27,152.62       | \$109,515.34     |
| 48.86 | 0.0420 | \$291.58        | \$3,468.00      | \$1,044.41      | \$42.39         | \$1,031.21        | \$5,877.59       |
| 49.86 | 0.0015 | \$0.35          | \$120.79        | \$1.27          | \$0.00          | \$1.25            | \$123.66         |
|       |        |                 |                 |                 |                 | ΣC <sub>d</sub> = | <b>\$158,595</b> |

demand scenario of the life-cycle of the 8-story building is shown in Table 7. The life-cycle cost is obtained as sum of the initial cost plus the damage cost, resulting in  $C_t = 0$ .

The damage cost for the simulated structural demand scenario of the life-cycle of the 12-story building is shown

in Table 8. The life-cycle cost of the 12-story structure is obtained from the sum of the costs associated with damage during the useful life of the structure and the initial cost, for this scenario of simulated demands, the total cost is:  $C_t =$  .

TABLE 7: Expected damage cost in the life-cycle of the 8-story building.

| Year  | DI     | C <sub>PR</sub> | C <sub>PC</sub> | C <sub>PI</sub> | C <sub>PL</sub> | C <sub>PV</sub> | C <sub>d</sub>      |
|-------|--------|-----------------|-----------------|-----------------|-----------------|-----------------|---------------------|
| 0.50  | 0.0031 | \$8.6           | \$1,408.6       | \$19.6          | \$0.0           | \$19.4          | \$1,456.2           |
| 0.83  | 0.0033 | \$9.9           | \$1,507.5       | \$22.5          | \$0.0           | \$22.2          | \$1,562.0           |
| 2.64  | 0.0019 | \$3.3           | \$868.6         | \$7.5           | \$0.0           | \$7.4           | \$886.7             |
| 3.44  | 0.0018 | \$2.9           | \$822.5         | \$6.7           | \$0.0           | \$6.6           | \$838.7             |
| 5.21  | 0.0283 | \$738.3         | \$13,044.2      | \$1,682.8       | \$26.0          | \$1,661.6       | \$17,152.9          |
| 17.38 | 0.0396 | \$1,445.6       | \$18,252.4      | \$3,294.9       | \$99.9          | \$3,253.3       | \$26,346.0          |
| 19.84 | 0.0005 | \$0.3           | \$246.7         | \$0.6           | \$0.0           | \$0.6           | \$248.1             |
| 22.98 | 0.0009 | \$0.8           | \$422.6         | \$1.8           | \$0.0           | \$1.7           | \$426.9             |
| 23.66 | 0.0015 | \$2.0           | \$680.2         | \$4.6           | \$0.0           | \$4.5           | \$691.3             |
| 29.72 | 0.0010 | \$1.0           | \$480.7         | \$2.3           | \$0.0           | \$2.3           | \$486.3             |
| 34.72 | 0.4506 | \$187,193.8     | \$207,706.1     | \$426,679.5     | \$1,674,675.4   | \$421,289.8     | \$2,917,544.6       |
| 36.15 | 0.0004 | \$0.1           | \$183.3         | \$0.3           | \$0.0           | \$0.3           | \$184.1             |
| 37.42 | 0.0025 | \$5.9           | \$1,171.0       | \$13.6          | \$0.0           | \$13.4          | \$1,203.9           |
| 38.18 | 0.0025 | \$5.7           | \$1,145.5       | \$13.0          | \$0.0           | \$12.8          | \$1,177.0           |
| 38.39 | 0.0008 | \$0.5           | \$352.4         | \$1.2           | \$0.0           | \$1.2           | \$355.4             |
| 41.94 | 0.2557 | \$60,274.8      | \$117,861.4     | \$137,387.1     | \$173,627.9     | \$135,651.7     | \$624,802.9         |
| 43.56 | 0.0031 | \$8.8           | \$1,427.3       | \$20.1          | \$0.0           | \$19.9          | \$1,476.2           |
| 43.87 | 0.0002 | \$0.0           | \$80.0          | \$0.1           | \$0.0           | \$0.1           | \$80.1              |
| 48.03 | 0.1104 | \$11,231.6      | \$50,877.3      | \$25,600.7      | \$6,028.8       | \$25,277.3      | \$119,015.6         |
|       |        |                 |                 |                 |                 | $\Sigma C_d =$  | <b>\$ 3,715,935</b> |
|       |        |                 |                 |                 |                 |                 | <b>\$ 3.72 (MM)</b> |

TABLE 8: Expected damage cost in the life-cycle of the 12-story building.

| Year  | DI     | C <sub>PR</sub> | C <sub>PC</sub> | C <sub>PI</sub> | C <sub>PL</sub> | C <sub>PV</sub> | C <sub>d</sub>         |
|-------|--------|-----------------|-----------------|-----------------|-----------------|-----------------|------------------------|
| 2.19  | 0.0015 | \$4.48          | \$1,494.98      | \$7.09          | \$0.00          | \$7.00          | \$1,513.56             |
| 4.72  | 0.0027 | \$14.53         | \$2,690.96      | \$22.98         | \$0.00          | \$22.69         | \$2,751.16             |
| 5.5   | 0.0035 | \$24.42         | \$3,488.28      | \$38.61         | \$0.01          | \$38.12         | \$3,589.44             |
| 9.42  | 0.0604 | \$7,271.89      | \$60,197.78     | \$11,498.53     | \$1,029.06      | \$11,353.29     | \$91,350.56            |
| 12.63 | 0.0123 | \$301.57        | \$12,258.82     | \$476.85        | \$1.77          | \$470.82        | \$13,509.83            |
| 14.07 | 0.359  | \$256,899.01    | \$357,798.07    | \$406,216.42    | \$1,284,313.83  | \$401,085.26    | \$2,706,312.59         |
| 15.35 | 0.0022 | \$9.65          | \$2,192.63      | \$15.26         | \$0.00          | \$15.06         | \$2,232.60             |
| 16.02 | 0.0054 | \$58.12         | \$5,381.92      | \$91.91         | \$0.07          | \$90.75         | \$5,622.77             |
| 19.52 | 0.0019 | \$7.20          | \$1,893.64      | \$11.38         | \$0.00          | \$11.23         | \$1,923.45             |
| 19.98 | 0.0048 | \$45.93         | \$4,783.93      | \$72.62         | \$0.04          | \$71.70         | \$4,974.22             |
| 22    | 0.0037 | \$27.29         | \$3,687.61      | \$43.15         | \$0.01          | \$42.60         | \$3,800.67             |
| 23.56 | 0.0307 | \$1,878.67      | \$30,597.22     | \$2,970.61      | \$68.68         | \$2,933.08      | \$38,448.26            |
| 24.06 | 0.0028 | \$15.63         | \$2,790.63      | \$24.71         | \$0.00          | \$24.40         | \$2,855.37             |
| 25.73 | 0.0049 | \$47.86         | \$4,883.59      | \$75.68         | \$0.04          | \$74.72         | \$5,081.90             |
| 29.8  | 0.0027 | \$14.53         | \$2,690.96      | \$22.98         | \$0.00          | \$22.69         | \$2,751.16             |
| 30.25 | 0.0027 | \$14.53         | \$2,690.96      | \$22.98         | \$0.00          | \$22.69         | \$2,751.16             |
| 32.22 | 0.0053 | \$55.99         | \$5,282.26      | \$88.54         | \$0.06          | \$87.42         | \$5,514.26             |
| 32.62 | 0.0003 | \$0.18          | \$299.00        | \$0.28          | \$0.00          | \$0.28          | \$299.74               |
| 32.77 | 0.0045 | \$40.36         | \$4,484.93      | \$63.83         | \$0.03          | \$63.02         | \$4,652.17             |
| 33.06 | 0.0038 | \$28.78         | \$3,787.28      | \$45.51         | \$0.02          | \$44.94         | \$3,906.53             |
| 38.1  | 0.0019 | \$7.20          | \$1,893.64      | \$11.38         | \$0.00          | \$11.23         | \$1,923.45             |
| 40.81 | 0.0021 | \$8.79          | \$2,092.97      | \$13.90         | \$0.00          | \$13.72         | \$2,129.39             |
| 48.77 | 0.0058 | \$67.05         | \$5,780.58      | \$106.03        | \$0.09          | \$104.69        | \$6,058.44             |
| 48.77 | 0.0031 | \$19.16         | \$3,089.62      | \$30.29         | \$0.01          | \$29.91         | \$3,168.98             |
| 49.97 | 0.0047 | \$44.03         | \$4,684.26      | \$69.62         | \$0.04          | \$68.75         | \$4,866.70             |
|       |        |                 |                 |                 |                 | $\Sigma C_d =$  | <b>\$ 2,921,988.34</b> |
|       |        |                 |                 |                 |                 |                 | <b>\$ 2.92 (MM)</b>    |

## 5. Conclusions

In this paper, a general methodology to obtain the life-cycle costs for buildings located at the soft soil of Mexico City was presented. The costs considered in the analysis are the initial

costs and the cost due to damage. The structural damage was obtained by simulating the damage using the seismic demand hazard curve; however, the number of nonlinear analyses to obtain the curve can be complex and time demanding. This paper proposes a methodology to reduce the

analysis time by using ANNs. The proposed method uses ANNs to model a relationship between the parameters describing the structure and the seismic demand hazard curve. Two feedforward backpropagation network models were selected, the first model was used to obtain the structural design of the buildings, and the second model to obtain the seismic demand hazard curve. The analyzes were conducted considering 3D R/C buildings with varying story height, and bay length subjected to soft soil ground motion records. The performance of the ANN was evaluated by obtaining the seismic demand hazard curve for the different buildings and it was found to be capable of successfully predicting the curves. The accuracy of the developed model was tested by comparing the results of the traditional method and those obtained by the ANNs. The results show that the relative error of the seismic demand hazard curve for the different buildings were between 6% and 12%. It can be considered that the results were acceptable, taking into consideration the computational time reduced from about a few hours when obtaining an exact solution to a few seconds when the ANN model is used. A limitation in the applicability of the presented method is due to the nature of the ANNs that learn the relationships using examples data sets, the particular implementation proposed is then limited to the range of parameters, such as types of buildings, types of soil, properties of materials in construction, etc. Used for the training of the ANNs, any extension of its applicability in other types of buildings will require the generation of additional data to expand the parameters used in the training of the network. Based on the results obtained from the ANN, the seismic demand hazard curves were used to simulate demands in the life-cycle of the structures, from the simulated demands the damage scenario for the life-cycle of the structures was obtained. The total costs of the structures that are given by the initial costs and costs for damage during the useful life were obtained. The total cost obtained in the analysis for the 4-story building was \$323,586 US dollars, for the 8-story building the total cost obtained was \$4.64 million US dollars, and for the 12-story building the total cost during its life-cycle was \$4.91 million US dollars. The proposed approach to obtain the life-cycle cost would be of great use to investors and builders in helping them to consider the future costs of constructing buildings on soft ground in Mexico City. Finally, it is concluded that life-cycle cost is efficiently obtain using artificial neural networks models for the reliability analysis of reinforced concrete building, so it can be used as an excellent planning tool that covers long spans of time.

### Data Availability

The data used to support the findings of this study are available from the corresponding authors upon request.

### Conflicts of Interest

The authors declare that there is no conflict of interest regarding the publication of this paper.

### Acknowledgments

The first author would like to thank CONACYT (Consejo Nacional de Ciencia y Tecnología from México), for the scholarship provided to pursue his PhD studies. The second and sixth author appreciate the support of CONACYT under grant Ciencia Básica 287103. Thanks are given to the PASPA program of DGAPA-UNAM for the support provided to the fourth author. Financial support also was received from the Universidad Autónoma de Sinaloa under grant PROFAPI 2022.

### References

- [1] G. Barone and D. M. Frangopol, "Life-cycle maintenance of deteriorating structures by multiobjective optimization involving reliability, risk, availability, hazard and cost," *Structural Safety*, vol. 48, pp. 40–50, 2015.
- [2] P. Castaldo, B. Palazzo, and P. Della Vecchia, "Life-cycle cost and seismic reliability analysis of 3D systems equipped with FPS for different isolation degrees," *Engineering Structures*, vol. 125, pp. 349–363, 2016.
- [3] L. Ierimonti, L. Caracoglia, I. Venanzi, and A. L. Materazzi, "Investigation on life-cycle damage cost of wind-excited tall buildings considering directionality effects," *Journal of Wind Engineering and Industrial Aerodynamics*, vol. 171, pp. 207–218, 2017.
- [4] M. D. Pandey, J. A. M. van der Weide, and J. A. M. Van Der Weide, "Stochastic renewal process models for estimation of damage cost over the life-cycle of a structure," *Structural Safety*, vol. 67, pp. 27–38, 2017.
- [5] U. Vitiello, D. Asprone, M. Di Ludovico, and A. Prota, "Life-cycle cost optimization of the seismic retrofit of existing RC structures," *Bulletin of Earthquake Engineering*, vol. 15, no. 5, pp. 2245–2271, 2017.
- [6] O. Ei-Khoury, A. Shafieezadeh, and E. Fereshtehnejad, "A risk-based life cycle cost strategy for optimal design and evaluation of control methods for nonlinear structures," *Earthquake Engineering & Structural Dynamics*, vol. 47, no. 11, pp. 2297–2314, 2018.
- [7] P. Asadi and I. Hajirasouliha, "A practical methodology for optimum seismic design of RC frames for minimum damage and life-cycle cost," *Engineering Structures*, vol. 202, Article ID 109896, 2020.
- [8] M. Noureldin and J. Kim, "Parameterized seismic life-cycle cost evaluation method for building structures," *Structure and Infrastructure Engineering*, vol. 17, no. 3, pp. 425–439, 2020.
- [9] Y. K. Wen and Y. J. Kang, "Minimum building life-cycle cost design Criteria. I: Methodology," *Journal of Structural Engineering*, vol. 127, no. 3, pp. 330–337, 2001.
- [10] N. D. Lagaros, "Life-cycle cost analysis of design practices for RC framed structures," *Bulletin of Earthquake Engineering*, vol. 5, no. 3, pp. 425–442, 2007.
- [11] C. C. Mitropoulou, N. D. Lagaros, and M. Papadrakakis, "Life-cycle cost assessment of optimally designed reinforced concrete buildings under seismic actions," *Reliability Engineering & System Safety*, vol. 96, no. 10, pp. 1311–1331, 2011.
- [12] L. Esteva, D. Campos, and O. Díaz-L, "Life-cycle optimization in earthquake engineering," *Structure and Infrastructure Engineering*, vol. 7, no. 1-2, pp. 33–49, 2011.
- [13] A. H.-S. Ang, "Life-cycle considerations in risk-informed decisions for design of civil infrastructures," *Structure and Infrastructure Engineering*, vol. 7, no. 1-2, pp. 3–9, 2011.

- [14] D. De León, "Integrating Socio-Economics in the Development of Criteria for Optimal Aseismic Design of R/C Buildings," Ph. D Thesis, University of California, Irvine, EUA, 1996.
- [15] N. D. K. Reddy Chukka, L. Natrayan, and W. D. Mammo, "Seismic fragility and life cycle cost analysis of reinforced concrete structures with a hybrid damper," *Advances in Civil Engineering*, vol. 2021, Article ID 4195161, 17 pages, 2021.
- [16] H. Varae, A. Shishegaran, and M. R. Ghasemi, "The life-cycle cost analysis based on probabilistic optimization using a novel algorithm," *Journal of Building Engineering*, vol. 43, Article ID 1030322021, 2021.
- [17] H. Mirzaeefard, M. Mirtaheri, and M. A. Hariri-Ardebili, "Life-cycle cost analysis of pile-supported wharves under multi-hazard condition: aging and shaking," *Structure And Infrastructure Engineering*, vol. 2021, pp. 1–21, 2021.
- [18] H. Mohammadhassan, B. Behrouz, and R. Maknoon, "A risk-based framework for design of concrete structures against earthquake," *Computers and Concrete, An International Journal*, vol. 25, no. 2, pp. 167–179, 2020.
- [19] S. Shekhar, J. Ghosh, and J. E. Padgett, "Seismic life-cycle cost analysis of ageing highway bridges under chloride exposure conditions: modelling and recommendations," *Structure and Infrastructure Engineering*, vol. 14, no. 7, pp. 941–966, 2018.
- [20] N. Izeboudjen, C. Larbes, and A. Farah, "A new classification approach for neural networks hardware: from standards chips to embedded systems on chip," *Artificial Intelligence Review*, vol. 41, no. 4, pp. 491–534, 2014.
- [21] D. Wang, H. He, and D. Liu, "Intelligent optimal control with critic learning for a nonlinear overhead crane system," *IEEE Transactions on Industrial Informatics*, vol. 14, no. 7, pp. 2932–2940, 2017.
- [22] J. Bojórquez, S. E. Ruiz, B. Ellingwood, A. Reyes-Salazar, and E. Bojórquez, "Reliability-based optimal load factors for seismic design of buildings," *Engineering Structures*, vol. 151, pp. 527–539, 2017.
- [23] Z. Beljkaš, M. Knežević, S. Rutešić, and N. Ivanišević, "Application of artificial intelligence for the estimation of concrete and reinforcement consumption in the construction of integral bridges," *Advances in Civil Engineering*, vol. 2020, Article ID 8645031, 8 pages, 2020.
- [24] H. H. Elmousalami, "Artificial intelligence and parametric construction cost estimate modeling: state-of-the-art review," *Journal of Construction Engineering and Management*, vol. 146, no. 1, Article ID 03119008, 2020.
- [25] T. García-Segura, V. Yepes, and D. M. Frangopol, "Multi-objective design of post-tensioned concrete road bridges using artificial neural networks," *Structural and Multidisciplinary Optimization*, vol. 56, no. 1, pp. 139–150, 2017.
- [26] O. R. De Lautour and P. Omenzetter, "Prediction of seismic-induced structural damage using artificial neural networks," *Engineering Structures*, vol. 31, no. 2, pp. 600–606, 2009.
- [27] P. Alvanitopoulos, I. Andreadis, and A. Elenas, "A New Algorithm for the Classification of Earthquake Damages in structures," in *Proceedings of the 5th IASTED International Conference on Signal Processing, Pattern Recognition and Applications*, pp. 151–156, Innsbruck, Austria, February 2008.
- [28] M. P. González and J. L. Zapico, "Seismic damage identification in buildings using neural networks and modal data," *Computers & Structures*, vol. 86, no. 3-5, pp. 416–426, 2008.
- [29] T. A. Reddy, K. R. Devi, and S. V. Gangashetty, "Multilayer feedforward neural network models for pattern recognition tasks in earthquake engineering," in *Proceedings of the International Conference on Advanced Computing, Networking and Security*, pp. 154–162, Springer, Urathkal, India, December 2011.
- [30] M. A. Orellana, S. E. Ruiz, J. Bojórquez, A. Reyes-Salazar, and E. Bojórquez, "Optimal load factors for earthquake-resistant design of buildings located at different types of soils," *Journal of Building Engineering*, vol. 34, Article ID 102026, 2021.
- [31] J. P. Wang, D. Huang, S.-C. Chang, and Y.-M. Wu, "New evidence and perspective to the Poisson process and earthquake temporal distribution from 55,000 events around Taiwan since 1900," *Natural Hazards Review*, vol. 15, no. 1, pp. 38–47, 2014.
- [32] D. Vamvatsikos and C. A. Cornell, "Incremental dynamic analysis," *Earthquake Engineering & Structural Dynamic*, vol. 31, no. 3, pp. 491–514, 2001.
- [33] L. Esteva, "Bases para la formulación de decisiones de diseño sísmico," PhD thesis, Facultad de Ingeniería, Universidad Nacional Autónoma de México, México, North America, 1968.
- [34] C. A. Cornell, "Engineering seismic risk analysis," *Bulletin of the Seismological Society of America*, vol. 58, no. 5, pp. 1583–1606, 1968.
- [35] Matlab, *Matlab Toolbox, Windows*, The MathWorks, Inc, Natick, Massachusetts, 2015.
- [36] R. Y. Rubinstein, *Simulation and the Monte Carlo Method*, p. 372, John Wiley & Sons, Hoboken Nj, USA, 1981.
- [37] B. Behnam and F. Shojaei, "A Risk Index for Mitigating Earthquake Damage in Urban Structures," *Integrating Disaster Science and Management*, vol. 2018, pp. 3–25, 2018.
- [38] A. D'Ambrisi, M. De Stefano, M. Tanganelli, and S. Viti, "In Book: Seismic Behaviour and Design of Irregular and Complex Civil Structures; Chapter," *The Effect of Common Irregularities on the Seismic Performance of Existing RC Framed Buildings*, Springer, Dordrecht, NY, USA, 2013.
- [39] D. Tolentino and S. E. Ruiz, "Time intervals for maintenance of offshore structures based on multiobjective optimization," *Mathematical Problems in Engineering*, vol. 2013, Article ID 125856, 15 pages, 2013.
- [40] D. De León and A. H. S. Ang, "A Damage Model for Reinforced Concrete Buildings, Further Study with the 1985 Mexico City Earthquake," in *Structural Safety And Reliability*, G. Schueller et al., Ed., pp. 2081–2087, AA Balkema, Rotterdam, Netherlands, 1995.
- [41] A. Surahman and K. B. Rojiani, "Reliability based optimum design of concrete frames," *Journal of Structural Engineering*, vol. 109, no. 3, pp. 741–757, 1983.
- [42] D. P. Rice and B. S. Cooper, "The economic value of human life," *American Journal of Public Health and the Nations Health*, vol. 57, no. 11, pp. 1954–1966, 1967.
- [43] W. K. Viscusi and E. P. Gentry, "The value of a statistical life for transportation regulations: A test of the benefits transfer methodology," *Journal of Risk and Uncertainty*, vol. 51, no. 1, pp. 53–77, 2015.
- [44] W. K. Viscusi and J. E. Aldy, "The value of a statistical life: a critical review of market estimates throughout the world," *Journal of Risk and Uncertainty*, vol. 27, no. 1, pp. 5–76, 2003.
- [45] T. R. Miller, "Variations between countries in values of statistical life," *Journal of Transport Economics and Policy*, vol. 34, no. 2, pp. 169–188, 2000.
- [46] R. Meli and E. Miranda, *Evaluación de los Efectos de los sismos de septiembre de 1985 en los edificios de la Ciudad de México*, Parte I: Evaluación de daños, Instituto de Ingeniería, México, North America, 1986.

- [47] T. M. Government, "Report in the Investigation of the Earthquake in Mexico," 1985, <https://www.nist.gov/el/earthquake-mexico-1985>.
- [48] Inegi, "Encuesta nacional de ingresos y gastos de los hogares," 2020, <https://www.inegi.org.mx/programas/enigh/nc/2020/>.
- [49] Iingen, "Red Acelerográfica del Instituto de Ingeniería (RAII-UNAM)," Instituto de ingeniería, Universidad Nacional Autónoma de México, 2020, <http://aplicaciones.iingen.unam.mx/AcelerogramasRSM/>.
- [50] Reglamento de construcción del Distrito Federal, *Administración Pública de la Ciudad de México*, Gaceta Oficial de la Ciudad de México, Jefatura de Gobierno, Ciudad de México, México, North America, 2021.
- [51] A. J. Carr, *User Manual for the 3-dimensional Version, ruaumoko3D*, Department of Civil Engineering, University of Canterbury, Christchurch, New Zealand, 2007.
- [52] H. Reyes, *Análisis de sensibilidad de factores de carga, muerta, viva y sismos en edificios desplantados en diferentes tipos de suelo*, Universidad Autónoma de Sinaloa, MC. Thesis, 2019.
- [53] J. Bojórquez, "Combinación óptima para diseño sísmico de edificios," Ph.D. Thesis in Spanish, Universidad Nacional Autónoma de México, Culiacán, Mexico, 2016.
- [54] J. Bojórquez, D. Tolentino, J. Yunes, and S. E. Ruiz, *Diseño de edificios de concreto reforzado utilizando redes neuronales artificiales*, XIX Congreso Nacional de Ingeniería Estructural Puerto Vallarta, Puerto Vallarta, Mexico, in Spanish, 2014.